Advanced Matrix Phased Array Settings for Inspection

Frederic REVERDY [1], Steve MAHAUT [1], Philippe DUBOIS [1], Laurent LE BER [2], Olivier ROY [2]
[1]CEA, Saclay bâtiment 611, Gif sur Yvette, F-91191 France
Phone : +33 169083767, Fax : +33 169087597, e-mail : frederic.reverdy@cea.fr
[2]M2M, Les Ulis, 91940, France, e-mail : l.leber@m2m-ndt.com

Abstract

Phased-array technology is being more and more adopted in the field of ultrasonic non destructive testing because of its enhanced flexibility over conventional monolithic probes. The most common abilities of steering, focusing and electronic scanning have been largely described; they allow faster inspection times or inspection of components with limited accessibility. Although these techniques have been used for quite some time in the NDT field, most applications have been carried out with linear phased-array probes (1D probe). More complex applications now require advanced phased-array techniques based on matrix array design. The use of matrix array probes usually leads to an increase in the number of elements and requires improved phased-array driving software and systems. Recent developments carried out at CEA and M2M are providing user-friendly tools to conceive and exploit these 2D probes. By defining groups of transmitters and receivers, electronic trajectories, active apertures (patterns) and combining them with advanced delay laws it is now possible to predict complex inspections. It is also possible to visualize the simulated or acquired data resulting from those inspections in a 3D view of the component thanks to 3D-CAD features and ultrasonic ray paths. Several inspections of complex components (nozzles, CAD specimen…) are presented here; they illustrate some potential applications for matrix array probes.

Keywords: Phased-array techniques, 2D array probes

1. Introduction

The recent developments in commercial acquisition systems and probes have led to a wider implementation of the phased-array technology in various industrial fields. While regular operating modes such as focusing, steering and various electronic scanning or any combination of those have been implemented for a long time, they have been usually limited to 1D probes such as linear or circular arrays. However, the ever-increasing number of UT channels available within the acquisition systems enables the use of these techniques with matrix array probes. While 3D beam sweeping, focusing and electronic scanning offer new inspection possibilities; it is crucial to conceive simulation tools and user-friendly interfaces that will help users exploit these tools to their full potential.

Designing a matrix array probe and predicting its performances and limitations is the first step for an inspection procedure qualification. To assess these performances, the French Atomic Commission (CEA) has developed for years semi-analytical models dedicated to UT. These simulations tools, gathered in the CIVA software[1], can calculate delay laws, beam propagation, flaw scattering and offer various imaging tools. All these calculations are available for simple (circular or linear probes) or more sophisticated (1.5D, 2D matrix or sectorial array probes).

The simulation tools used in CIVA and their related configurations are first briefly introduced. Various applications of simulations using matrix phased-array probes are then

presented. Finally, some data reconstruction based on processing the collection of data acquired for each channel of an array is explained.

2. Modeling of phased-array techniques in CIVA

2.1 Beam propagation and flaw response computation

UT semi-analytical models developed in the CIVA platform aim at fully predict an inspection. To simulate the inspection, various flaw scattering approximations may be involved[2-3] depending on the configuration cases (type of inspection: pulse echo, tandem or TOFD technique) and on the flaw type (volumetric void flaws, crack-like flaws, solid inclusions), while the field incident over the flaw is modeled using a surface integral over the transducer aperture[4]. Finally, the synthesis of the signal at reception is computed using an argument based on Auld's reciprocity[5]. This calculation is done for each scanning position of the probe, for each applied parameters (delay and amplitude law) over the array, and for each elementary mode contribution: direct specular echoes in longitudinal and transverse modes, corner echoes with or without mode conversion occurring over the flaw or over the backwall, then the overall echo at reception is the sum of all these elementary modes.

2.2 Delay laws and operating modes

Because matrix array probes can perform full 3D volumetric inspections, it is necessary to develop user-friendly interfaces that allow the calculation of the most complex delay laws. One can now use the recent developments brought to CIVA to define the pattern of the active source and reception. This pattern can be of any shape; a square and ring patterns are shown as example in red in Figure 1. These patterns can then be electronic scanned across the full aperture of the array. Two trajectories are presented in Figure 1, a crenel-like displacement and a displacement along the diagonal of the array. It is possible to assign two totally different trajectories for the source and reception for tandem

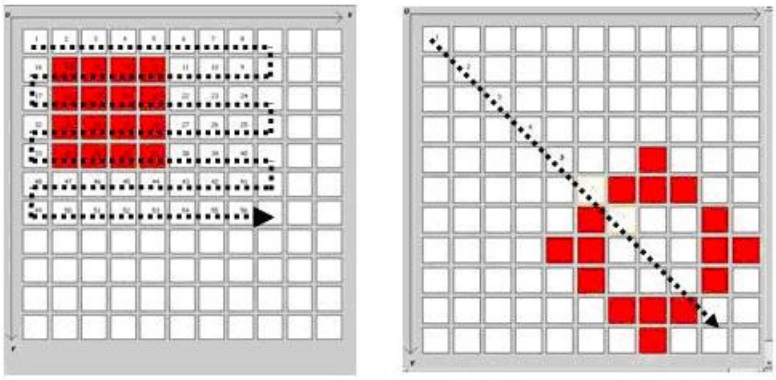

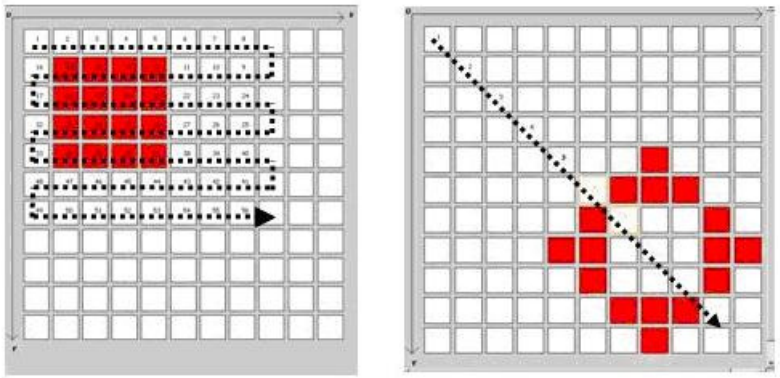

application. After defining the patterns and trajectories, one can calculate delay laws to focus and/or deflect the beam in 2 or 3 dimensions according to the symmetry of the array. The delay law calculations take into account arbitrary component shapes (canonical or CAD defined) and structures (homogeneous or heterogeneous, each medium being isotropic or anisotropic). The new interface is available for linear, matrix, circular, sectorial, encircling or encircled arrays and various operating probes (contact, immersion, flexible, dual T/R probes).

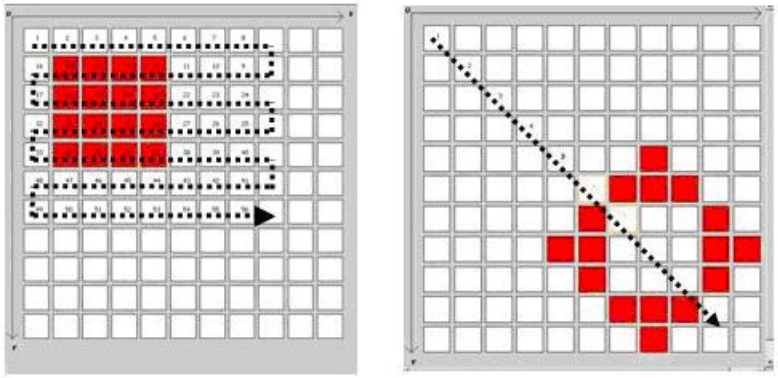

Figure 1 : Patterns (red elements) and trajectories across a matrix array probe (arrow).

Finally, a dynamic depth focusing delay law algorithm has been implemented to homogenize the beam spot within a desired inspection range of depths, with fixed or optimal aperture of the array pattern.

2.3 Imaging and reconstruction tools

For each applied delay and amplitude laws, it is possible thanks to the simulation tools available in CIVA to determine the UT paths, time of flights and the amplitude of the radiated or scattered field inside a component. The knowledge of these quantities allow to build true scan images (display of the ultrasonic information in the frame of the specimen); some of these images are shown later in this paper when dealing with phased-array applications.

Figure 2 shows some of the field imaging tools available in CIVA to measure the focal spot dimensions and to evaluate the refraction angles; both features rely on a complete beam propagation. A simpler (and very fast) ray tracing tool is also illustrated showing the UT paths used to focus on a side-drilled hole.

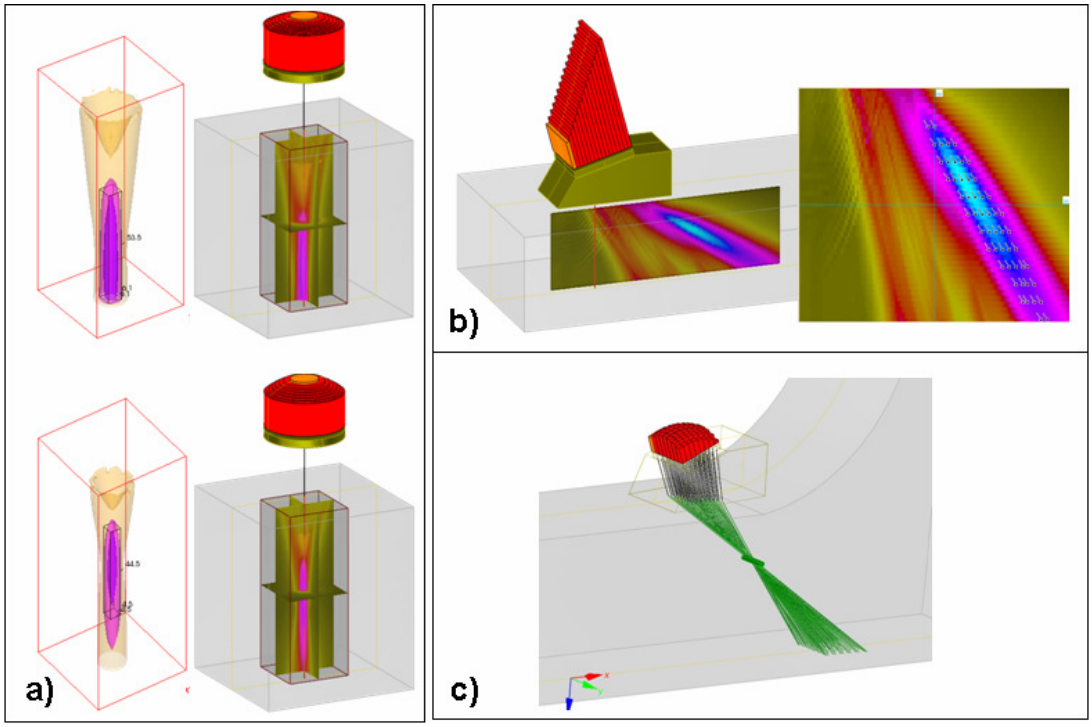

Figure 2 : a) measurement of the focal spot, b) estimation of the refraction angle, and c) ray tracing tool.

3. Examples of simulation of phased-array techniques

The following examples illustrate some phased-array simulations, including beam propagation, flaw scattering and data reconstruction.

3.1 Designing matrix array patterns for 3D applications

The first step when conceiving an inspection based on phased-array methods is to design the array pattern and one important goal is to minimize the amount of grating lobes generated by the array. It is well known that grating lobes occur if the elements are not thin enough to create destructive interferences outside of the desired focusing area.

Empiric rules may be used at first glance to check the validity of the array pattern. The main criterion used is the ratio between the wavelength and the elements “pitch” (distance center to center between two adjacent elements). One usually considers that:

- If the pitch is lower than half a wavelength, no grating lobe occurs.
- If the pitch is between half a wavelength and one wavelength, grating lobes occur, their amplitudes and positions depends on the applied delay law and the symmetry of the array design.
- If the pitch is higher than one wavelength, grating lobes, greater than the main lobe, may be generated.

Any phased-array design stage needs to find a compromise between the number of elements, imposed by the cost of the equipment and the space available to position the probe and the required performances of the inspection (spatial resolution, refraction angles, 2D or 3D steering…). Simulation constitutes the most versatile tool to conceive an array design from scratch and to check its performances.

Figure 2 shows some transmitted beams obtained by two 2D-array probes: one 2D matrix array (8x8 elements) and one sectored array (6 rings), divided into 61 elements, each ring

being divided by an increasing number of sectors. These probes have the same active aperture (about 256 mm²). They are used at the same frequency of 3 MHz and both share almost the same number of elements. The delay laws are calculated to perform a 3D steering of the beam in a planar specimen. The beam fields are displayed as iso-amplitude 3D curves (from 0 to -20 dB). It is possible to see the main lobe and the grating lobes generated by the arrays. The overall spatial distribution of those grating lobes, as expected, depends on the symmetry of the array showing that arrays with similar aperture, number of elements and central frequency can have totally different performances.

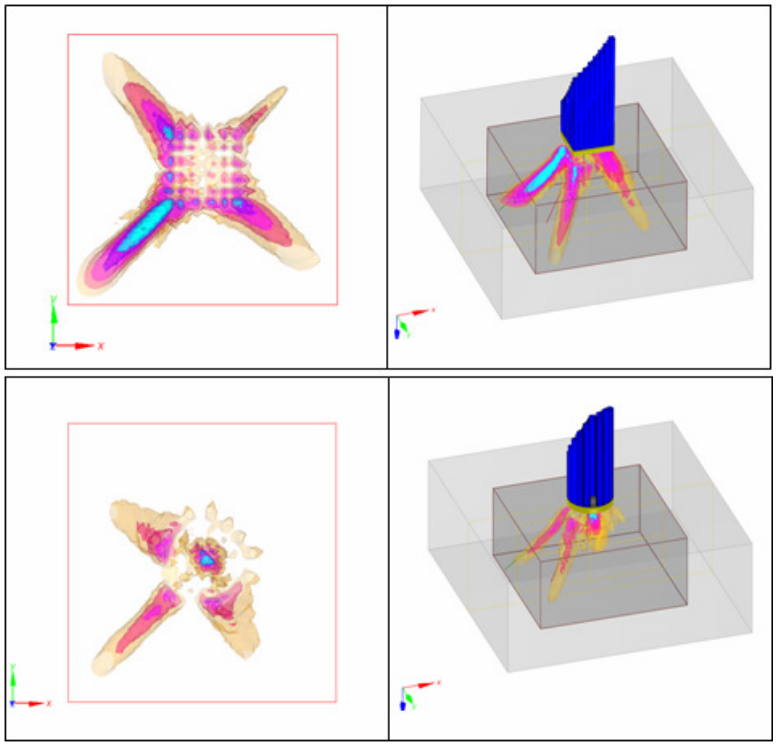

Figure 3: Example of 3D beam computation with 2D array patterns (2D matrix array of 8x8 elements, top view, and sectored arrays of 61 elements, bottom view).

Still, it has to be pointed out that the simulation of the grating lobes through beam simulation is not enough to predict *in fine* the performances of the inspection, as those grating lobes will also be scattered by flaws and boundaries of the specimen. The application of delay laws at reception over the echoes caused by the grating lobes should also be taken into account.

3.2 Focusing and deflection through a bimetallic weld

The following example shows delay law and beam field calculations in a component presenting a complex geometry and structure. The component is a bimetallic weld in a pipe, which can be described by a set of homogeneous isotropic and anisotropic media. The component is defined as a 2.5D-CAD specimen (complex profile and revolution extrusion to form a 3D part). This component is made of two isotropic parts (stainless and ferritic steel), connected by an anisotropic austenitic weld. An anisotropic cladding also lies over the ferritic steel part.

The figure below shows the ray tracing and full beam computation radiated by a matrix array (11x11 elements, 1.5-MHz central frequency, spherically focused) for two different

configurations: no delay law (top views) and focalization of a 40°-longitudinal wave inside the weld. The ray tracing tools allow to quickly visualize the concentration of energy in the component by analyzing the concentration of rays. When no delay law is applied the beams seems to concentrate close to the surface, while when the focalization delay law is applied the rays concentrate at the requested focal zone. Although the ray tracing tools may indicate intuitively where the beam would be focused, it cannot be used to quantitatively predict the position and the amplitude of the focal area. A full beam field calculation is then necessary to predict the characteristics of the beam.

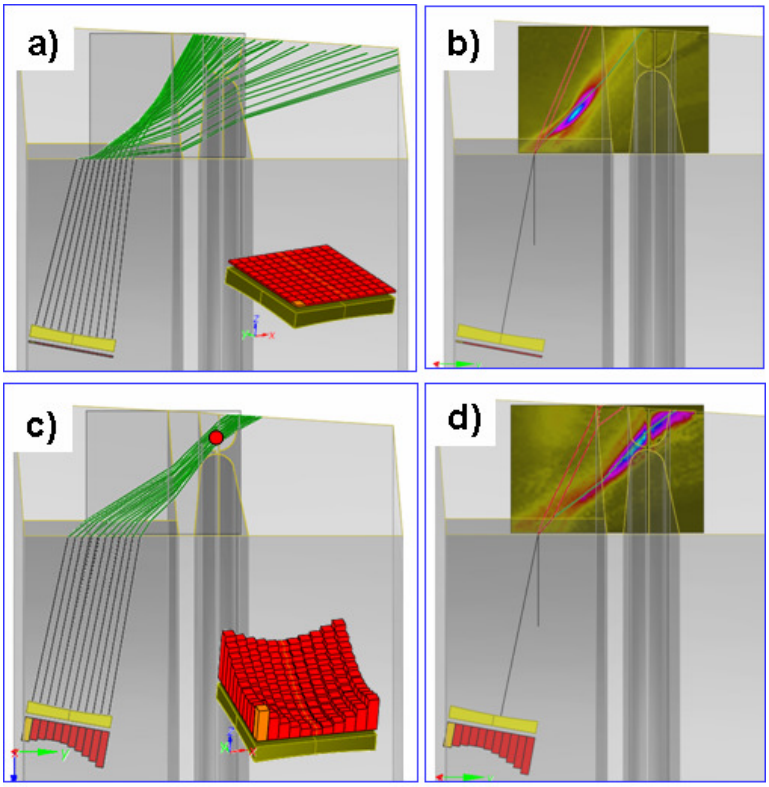

Figure 4: Example of ray tracing and beam computation for a matrix array used to focus through a bimetallic weld.

In this particular example, it is possible to focus the beam at the root of the weld despite the complexity of the structure using a matrix array probe and adapted delay laws to detect potential flaws in this area.

3.3 Combination of electronic and sectorial scannings for inspection of turbine blade attachment

The following example deals with another complex geometry, representative of turbine blade root attachment. The profile, displayed in the figure below, exhibits a complex geometry, which prevents a conventional probe to easily scan the component. One way to overcome such restriction is to use a phased-array probe working in a sectorial scanning operating mode. Delay laws are calculated to sweep the beam for a given arbitrary range of refraction angles (the beam may be, in addition, focused). In this example, a flexible matrix array of 8x8 elements is used to sweep longitudinal waves from 30° to 60°, with a reduced number of elements (8 rows, 2 columns). It is combined to an electronic commutation along the direction perpendicular to the complex profile to inspect a full volume of the component

without displacement of the probe. During this inspection, seven sectorial scans are recorded to provide a 3D scan of the component. Figure 5 shows the inspection procedure and a superimposition of three simulated sectorial scan upon a 3D view of the specimen. The simulation shows backwall echoes due to the complex profile as well as a corner echo coming from a crack-like flaw.

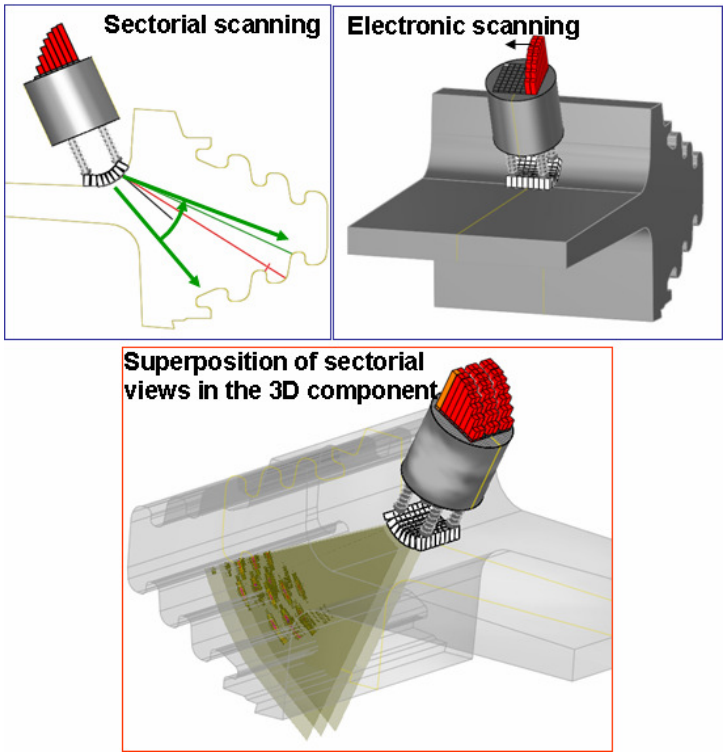

Figure 5: Illustration of a phased-array inspection combining electronic scanning and sectorial scanning in a turbine blade attachment.

4. Reconstruction of phased-array data

New tools dedicated to phased-array data processing (both simulated and experimental using phased-array acquisition systems developed by M2M[6]) have been added to the CIVA platform since version 9. These tools allow to post-process the data acquired by each channel during a phased-array inspection[7]. The post-processing technique consists in summing (after application of time delays and amplitude corrections calculated using model-based delay and amplitude laws) the contributions from each element of the array to synthetically focus the energy in various points of a reconstruction area in the component. Basically, the technique relies on the calculation of UT propagation paths from the transmitting element to any point of a reconstruction area to the receiving element. Those paths are modeled using the previously detailed simulation tools for beam computation and flaw scattering.

The first application of this technique is the case of a matrix array probe (11x11 elements, pitch 6.5 mm, 1-MHz central frequency) in contact with a ferritic steel specimen (220 mm thick) containing various flat-bottom holes (FBH, 2 mm in diameter) of different height (5

mm to 60 mm). The position of the probe over the flat-bottom holes is shown in

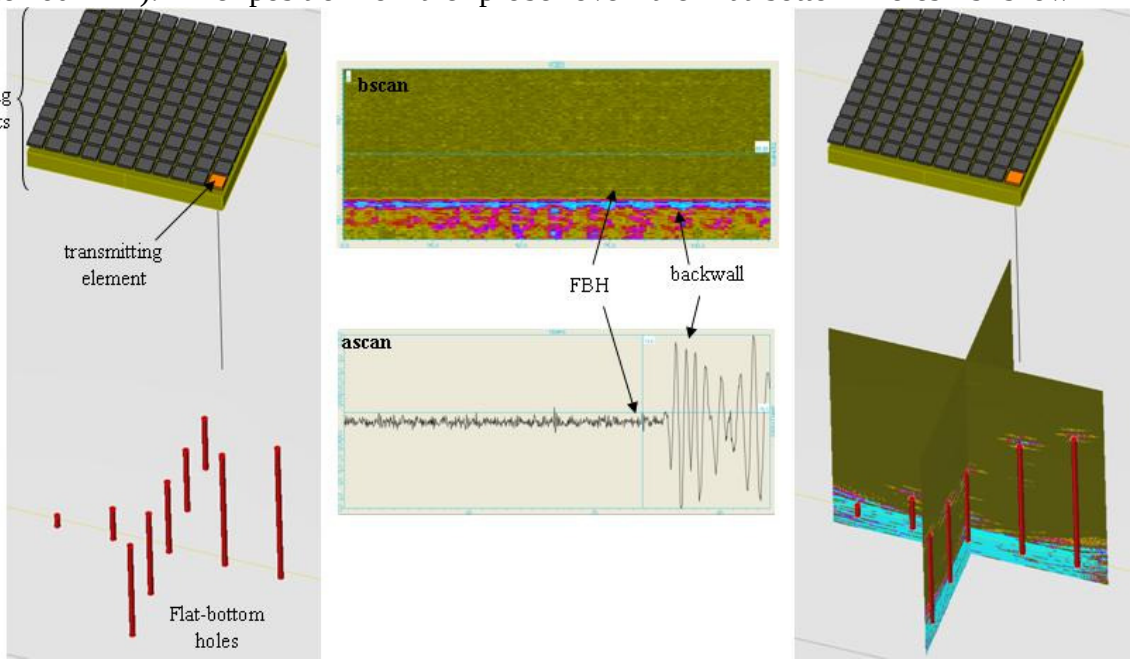

Figure 6. The acquisition scheme used here is referred to as Full Matrix Capture (FMC). It can be explained as follow: an electronic commutation is performed for which each element of the array is successively being used as a source while all the elements are used as receivers. A set containing all combinations of transmitter and receiver elements (121x121 signals for one mechanical position of the probe) is being stored for post-processing. A bscan and ascan from this set are shown in Figure 6; the signal-to-noise ratio associated with the FBH is relatively weak, which can be explained by the relatively long ultrasonic path and the small size of the sources and receivers (one element).

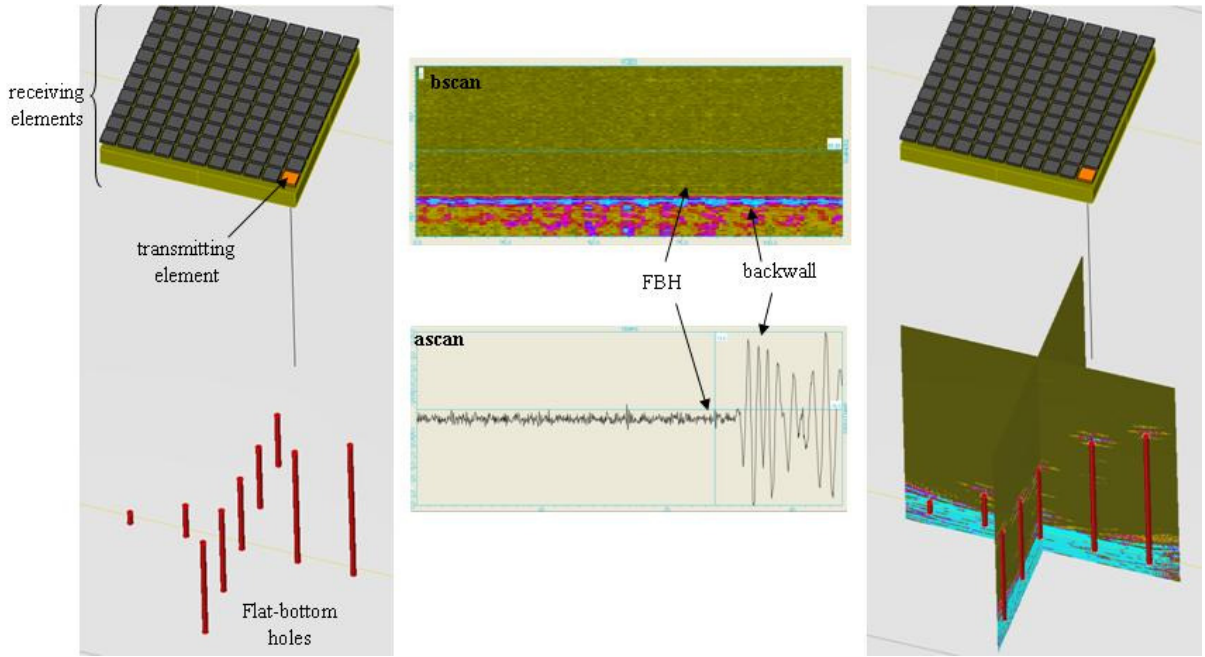

Figure 6 : Inspection configuration, examples of signals acquired during the FMC, and reconstruction result.

The reconstruction algorithm described before is used for experimental data along two perpendicular planes containing the holes.

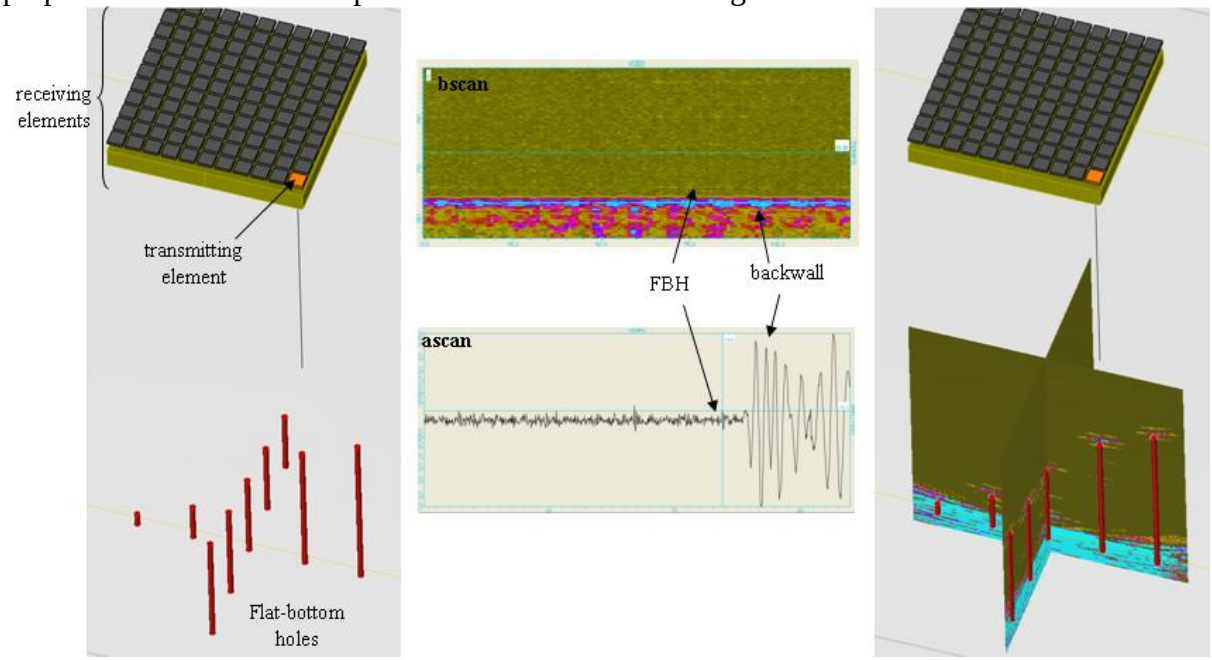

Figure 6 shows the superimposition of the two reconstructions upon a 3D view of the component containing the flat-bottom holes. It is important to notice that despite the poor signal-to-noise ratio observable in the individual ascans, the reconstruction technique leads to a clear detection of all the holes. The FMC acquisition combined with the reconstruction method presented here allows the detection of the defects without having to scan the specimen in all directions.

The second example deals with a 64-element linear array over a ferritic steel of complex profile, containing 8 side-drilled holes (4 side-drilled holes are located below a planar part, while the 4 other reflectors are located below a complex part). The reconstruction images (Figure 7) show excellent results in terms of positioning of the echoes (the reported circles correspond to the exact positions of the side-drilled hole in the component), resolution, and signal-to-noise ratio despite the surface irregularity.

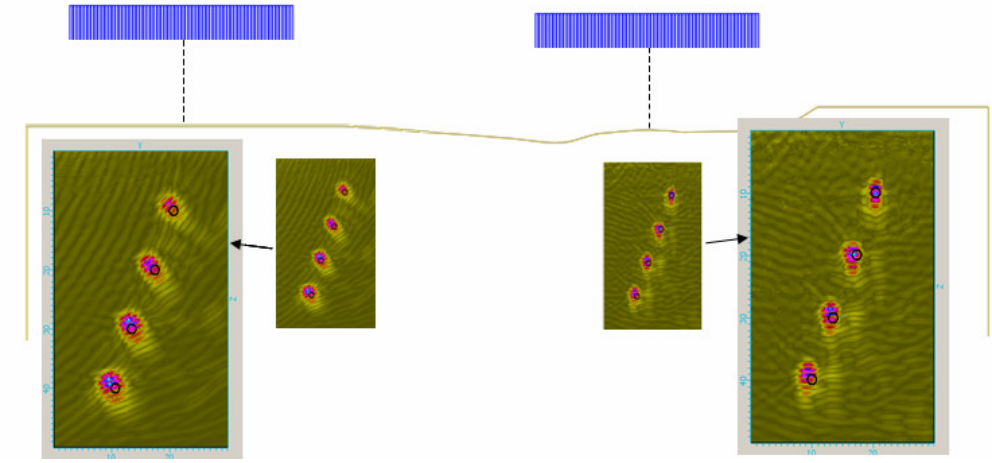

Figure 7: Reconstruction over planar and irregular parts of the component.

Conclusion

This paper has presented some of the phased-array simulation tools available in the CIVA platform. Those tools including delay computation, ray tracing, beam computation, flaw scattering and post-processing reconstructions, based on semi-analytical approach provide fast and accurate results. The recent developments in CIVA9 were aimed at extending those tools to 2D array probe. A user-friendly interface allows now to fully define and simulate complex inspection based on 2D array probes (combination of electronic scanning with arbitrary patterns and trajectories, fixed or variables patterns apertures along the trajectory…).

REFERENCES

[1] More details may be found at http://www-civa.cea.fr.

[2] Raillon R and Lecœur-Taïbi I, "Transient Elastodynamic Model for Beam Defect Interaction. Application to NonDestructive Testing", *Ultrasonics*, Volume 38, 2000, P527-530.

[3] Darmon M, Calmon P, Bèle B,"An integrated model to simulate the scattering of ultrasounds by inclusions in steels", *Ultrasonics*, Volume 42, 2004, P237-241

[4] Gengembre N, "Pencil method for ultrasonic beam computation", in *proceedings of the 5th World Congress on Ultrasonic*s, 2003, P1533-1536.

[5] Auld B, *Wave Motion* **1**, 3 (1979).

[6] O. Roy, M. Bouhelier,*"3D beam steering for improved detection of skewed crack"*, EPRI Piping & Bolting/Phased Array Inspection Conference, 2005

[7] Calmon P, Iakovleva E, Fidahoussen A, Ribay G, Chatillon S, *"Model based reconstruction of UT Array Data"*, to be published in proceedings of the 34th Review of Progress in QNDE, 2007